

based on an approximation that is valid so long as the synthesized field is not too large. If  $\xi$  and  $\eta$  are small enough that the term

$$\left(\sqrt{1 - \xi^2 - \eta^2} - 1\right)w \approx -\frac{1}{2}(\xi^2 + \eta^2)w \quad (4.4)$$

can be neglected, Eq. (4.3) becomes

$$\mathcal{V}(u, v, w) = \mathcal{V}(u, v, 0) = \int_{-\infty}^{\infty} \int_{-\infty}^{\infty} \frac{A_N(\xi, \eta) B(\xi, \eta)}{\sqrt{1 - \xi^2 - \eta^2}} e^{-j2\pi(u\xi + v\eta)} d\xi d\eta. \quad (4.5)$$

Thus for a restricted range of  $\xi$  and  $\eta$ ,  $\mathcal{V}(u, v, w)$  is approximately independent of  $w$ , and for the inverse transform we can write

$$\frac{A_N(\xi, \eta) B(\xi, \eta)}{\sqrt{1 - \xi^2 - \eta^2}} = \int_{-\infty}^{\infty} \int_{-\infty}^{\infty} \mathcal{V}(u, v) e^{j2\pi(u\xi + v\eta)} du dv. \quad (4.6)$$

With the above approximation it is usual to omit the  $w$  dependence and write the visibility as the two-dimensional function  $\mathcal{V}(u, v)$ . Note that the factor  $\sqrt{1 - \xi^2 - \eta^2}$  in Eqs. (4.5) and (4.6) can be absorbed into the function  $A_N(\xi, \eta)$ , if desired. The approximation in Eq. (4.5) introduces a phase error equal to  $2\pi$  times the neglected term, that is, approximately  $\pi(\xi^2 + \eta^2)w$ . Limitation of this error to some tolerable value places a restriction on the size of the synthesized field, which can be roughly estimated as follows. If the antennas track the source under observation down to low elevation angles, the values of  $w$  can approach the maximum spacings  $(D_N)_{\max}$  in the array, as shown in Fig. 4.3. Also if the spatial frequencies measured are evenly distributed out to the maximum spacing, the synthesized beamwidth  $\theta_b$  is approximately equal to  $(D_N)_{\max}^{-1}$ . Thus the maximum phase error is approximately  $\pi(\theta_b/2)^2 \theta_b^{-1}$ , where  $\theta_b$  is the width of the synthesized field. The condition that

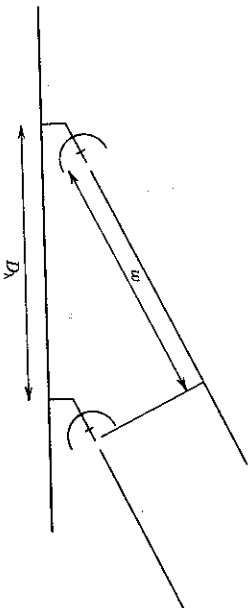


Figure 4.3 When observations are made at a low angle of elevation, and at an azimuth close to that of the baseline, the spacing component  $w$  becomes comparable to the baseline length  $D_N$ .

no phase errors can exceed, say, 0.1 rad then requires that

$$\theta_b < \frac{1}{3}\sqrt{\theta_b}, \quad (4.7)$$

where the angles are measured in radians. For example, if  $\theta_b = 1$  arcsec,  $\theta_b < 2.5$  arcmin. Most synthesis mapping in astronomy has been performed within this restriction, but ways of obtaining larger maps will be discussed.

We now return to the case of arrays with east-west spacings only, and discuss further the conditions for which we can put  $w = 0$ , and the resulting effects. Let us first rotate the pole as shown in Fig. 4.4. We indicate by primes the quantities measured in this system. The  $(u', v')$  axes lie in a plane parallel to the earth's equator. The east-west antenna spacings contain components in this plane only (i.e.  $w' = 0$ ), and as the earth rotates the spacing vectors sweep out circles concentric with the  $(u', v')$  origin. From Eq. (4.3) we can write

$$\mathcal{V}(u', v') = \int_{-\infty}^{\infty} \int_{-\infty}^{\infty} A_N(\xi', \eta') B(\xi', \eta') e^{-j2\pi(u'\xi' + v'\eta')} \frac{d\xi' d\eta'}{\sqrt{1 - \xi'^2 - \eta'^2}}, \quad (4.8)$$

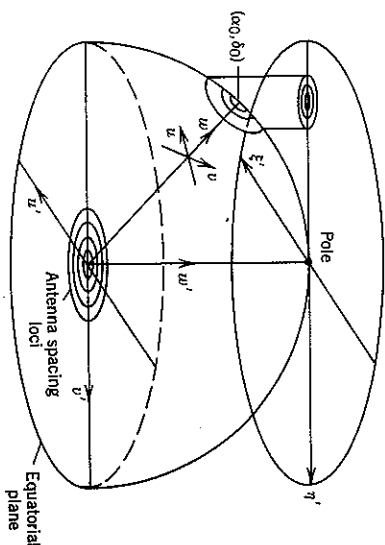


Figure 4.4 The  $(u', v')$  coordinate system for an east-west array. The  $(u', v')$  plane is the equatorial plane and the antenna-spacing vectors trace out arcs of concentric circles as the earth rotates. Note that the directions of the  $u'$  and  $v'$  axes are chosen so that the  $v'$  axis lies in the plane containing the pole, the observer, and the point under observation  $(\alpha_0, \delta_0)$ . In Fourier transformation from the  $(u', v')$  to the  $(\xi', \eta')$  planes the celestial hemisphere is mapped as a projection onto the tangent plane at the pole. The  $(u, v, w)$  coordinates for observation in the direction  $(\alpha_0, \delta_0)$  are also shown.

$(\xi, \eta, \zeta)$ . A two-dimensional brightness distribution can then be taken on the unit sphere in  $(\xi, \eta, \zeta)$ .

3. Most connected-element arrays are constructed on ground sufficiently flat that at any instant all the baselines are approximately in a plane, and they remain close to this plane for observations of short duration. As pointed out in the discussion of east-west baselines, visibility measurements made in a plane can be projected into the  $(u, v)$  plane with only a calculable distortion of the coordinates in the resulting map. It is therefore possible to divide a long observation into a series of shorter ones, to each of which a separate coordinate correction is applied before they are combined.

4. If the brightness distribution within the area to be mapped is known in advance to some degree of accuracy, this information can be used to derive  $\mathcal{V}(u, v, 0)$  from the measured  $\mathcal{V}(u, v, w)$  with improved accuracy. Thus a map with some distortion can be obtained from Eq. (4.6) and used to improve the estimation of  $\mathcal{V}(u, v, 0)$ . A more accurate map is then obtained, and, in principle, this process can be iterated until the desired accuracy is obtained.

Methods 1 to 3 above have been discussed by Clark (1982) and methods 3 and 4 by Bracewell (1979, 1984a). Up to the mid-1980s these methods have been little more than points for discussion, since most measurements have been performed within the restrictions for which Eq. (4.6) is adequate. Model calculations based on method 3 have been made by Hudson (1977).

## 4.2 ANTENNA SPACING COORDINATES AND $(u, v)$ LOCI

Various coordinate systems are used to specify the relative positions of the antennas in an array, and of these one of the more convenient for terrestrial arrays is shown in Fig. 4.5. A right-handed Cartesian coordinate system is used where  $X$  and  $Y$  are measured in a plane parallel to the earth's equator,  $X$  in the meridian plane (defined as the plane through the poles of the earth and the reference point in the array),  $Y$  toward the east, and  $Z$  is measured toward the north pole. In terms of hour angle  $H$  and declination  $\delta$ ,  $(X, Y, Z)$  are measured toward  $(H = 0, \delta = 0)$ ,  $(H = -6^\circ, \delta = 0)$  and  $(\delta = 90^\circ)$ , respectively. If  $(X_\lambda, Y_\lambda, Z_\lambda)$  are the components of  $\mathbf{D}_\lambda$  in the  $(X, Y, Z)$  system, the components  $(u, v, w)$  are given by

$$\begin{bmatrix} u \\ v \\ w \end{bmatrix} = \begin{bmatrix} \sin H & \cos H & 0 \\ -\sin \delta \cos H & \sin \delta \sin H & \cos \delta \\ \cos \delta \cos H & -\cos \delta \sin H & \sin \delta \end{bmatrix} \begin{bmatrix} X_\lambda \\ Y_\lambda \\ Z_\lambda \end{bmatrix} \quad (4.15)$$

Here  $(H, \delta)$  are usually the hour angle and declination of the phase reference position. (In VLBI observations it is customary to set the  $X$  axis in the Greenwich meridian, in which case  $H$  is measured with respect to that

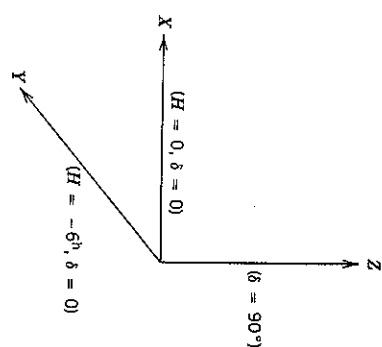


Figure 4.5 The  $(X, Y, Z)$  coordinate system for specification of relative positions of antennas. Directions of the axes are specified in terms of hour angle  $H$  and declination  $\delta$ .

meridian rather than a local one.) The elements of the transformation matrix above are the direction cosines of the  $(u, v, w)$  axes with respect to the  $(X, Y, Z)$  axes and can easily be derived from the relationships in Fig. 4.6. Another method of specifying the baseline vector is in terms of its length,  $D$ , and the hour angle and declination,  $(h, d)$ , of the intersection of the baseline direction with the northern celestial hemisphere. The coordinates in the

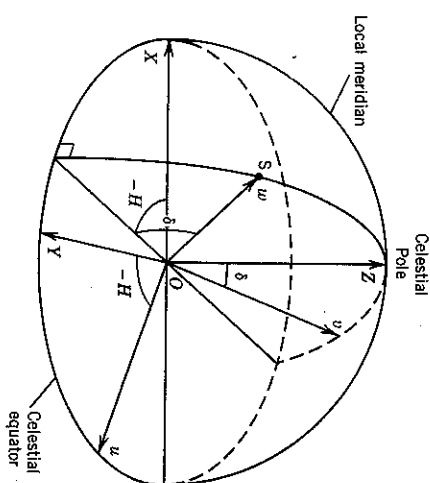


Figure 4.6 Relationships between the  $(X, Y, Z)$  and  $(u, v, w)$  coordinate systems. The  $(u, v, w)$  system is defined for observation in the direction of the point  $S$  which has hour angle and declination  $H$  and  $\delta$ . As shown  $S$  is in the eastern half of the hemisphere and  $H$  is therefore negative. The direction cosines in the transformation matrix in Eq. (4.15) follow from the relationships in this diagram. The relationship in Eq. (4.16) can also be derived if we let  $S$  represent the direction of the baseline and put the baseline coordinates  $(h, d)$  for  $(H, \delta)$ .

$(X, Y, Z)$  system are then given by

$$\begin{bmatrix} X \\ Y \\ Z \end{bmatrix} = D \begin{bmatrix} \cos d \cos h \\ \cdots \cos d \sin h \\ \sin d \end{bmatrix}. \quad (4.16)$$

The coordinates in the  $(u, v, w)$  system are, from Eqs. (4.15) and (4.16),

$$\begin{bmatrix} u \\ v \\ w \end{bmatrix} = D_\lambda \begin{bmatrix} \cos d \sin(H-h) \\ \sin d \cos \delta - \cos d \sin \delta \cos(H-h) \\ \sin d \sin \delta + \cos d \cos \delta \cos(H-h) \end{bmatrix}. \quad (4.17)$$

The  $(D, h, a)$  system was used more widely in the earlier literature, particularly for instruments involving only two antennas: see, for example, Rowson (1963) for an early application of Eq. (4.17) to a tracking interferometer.

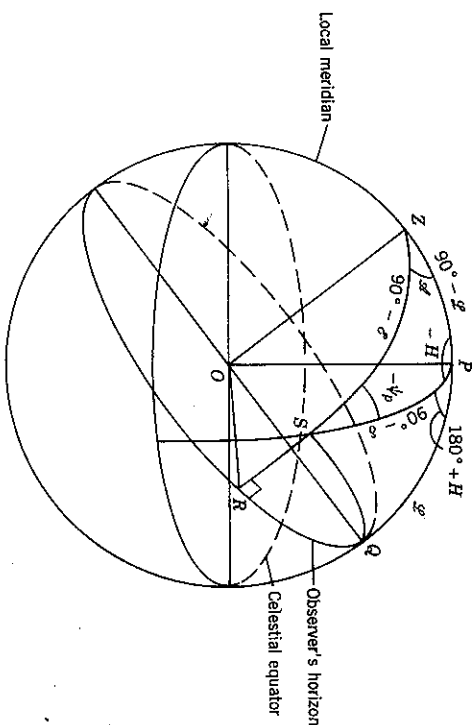


**Figure 4.7** Relationship between the celestial coordinates  $(H, \delta)$  and the elevation and azimuth  $(\mathcal{E}, \mathcal{A})$  of a point  $S$  as seen by an observer at latitude  $\mathcal{L}$ .  $P$  is the celestial pole and  $Z$  the observer's zenith. The parallactic angle  $\psi_p$  is the position angle of the observer's vertical on the sky measured from north toward east. The lengths of the arcs measured in terms of angles subtended at the center of the sphere  $O$  are as follows:

$$\begin{array}{ll} ZP = 90^\circ - \mathcal{Z} & PQ = \mathcal{Z} \\ SZ = 90^\circ - \mathcal{S} & SP = 90^\circ - \mathcal{S} \\ & SR = \mathcal{S} \quad RQ = \mathcal{A} \\ & SQ = \cos^{-1}(\cos \mathcal{S} \cos \mathcal{A}) \end{array}$$

The three equations in (A4.1) can be obtained by application of the sine and cosine rules for spherical triangles to  $ZPS$  and  $PQS$ . Note that with  $S$  in the eastern half of the observer's sky, as shown,  $H$  and  $\psi_p$  are negative.

When the  $(X, Y, Z)$  components of a new baseline are first established, the usual practice is to determine the elevation  $\mathcal{E}$ , azimuth  $\mathcal{A}$ , and length of the baseline by field surveying techniques. The relationship between  $(\mathcal{E}, \mathcal{A})$  and other coordinate systems is shown in Fig. 4.7 and Appendix 4.1. For latitude  $\mathcal{L}$ , using Eqs. (4.16) and (A4.2), we obtain

$$\begin{bmatrix} X \\ Y \\ Z \end{bmatrix} = D \begin{bmatrix} \cos \mathcal{L} \sin \mathcal{E} - \sin \mathcal{L} \cos \mathcal{E} \cos \mathcal{A} \\ \cos \mathcal{E} \sin \mathcal{A} \\ \sin \mathcal{L} \sin \mathcal{E} + \cos \mathcal{L} \cos \mathcal{E} \cos \mathcal{A} \end{bmatrix}. \quad (4.18)$$

Examination of Eqs. (4.15) or (4.17) shows that the locus of the projected antenna-spacing components  $u$  and  $v$  defines an ellipse with hour angle as the variable. Thus from Eq. (4.15),

$$u^2 + \left( \frac{v - Z_\lambda \cos \delta_0}{\sin \delta_0} \right)^2 = K_\lambda^2 + Y_\lambda^2, \quad (4.19)$$

where  $(H_0, \delta_0)$  is the phase reference position. In the  $(u, v)$  plane Eq. (4.19) defines an ellipse with the semimajor axis equal to  $\sqrt{X_1^2 + Y_1^2}$ , and the semiminor axis equal to  $\sin \delta_0 \sqrt{X_1^2 + Y_1^2}$  as in Fig. 4.8a. The ellipse is centered on the  $v$  axis at  $(u, v) = (0, Z_0 \cos \delta_0)$ . The arc of the ellipse that is traced out during any observation depends upon the azimuth, elevation, and latitude of the baseline, the declination of the source, and the range of hour angle covered,

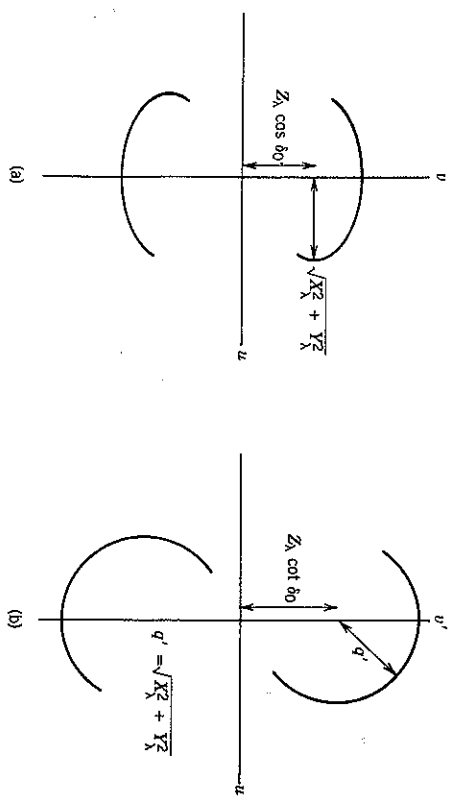


**Figure 4.8** (a) Spacing-vector locus in the  $(u, v)$  plane from Eq. (4.19), (b) Spacing-vector locus in the  $(u', v')$  plane from Eq. (4.22). The lower arc in each diagram represents the locus of conjugate values of visibility. Unless the source is circumpolar the cutoff at the horizon limits the lengths of the arcs.